Journal of the Korean Vacuum Society
Vol. 10. No. S1, June 2000, pp. 41~47

Medium-frequency microwave plasma immersion ion implantation

Tong Honghui, Xu Zej1i, Chen Qinchuan, Wang Ke, Huo Yanfeng, and Ma Di
Southwestern Institute of Physics, Chengdu610041, P.R.China

Paul.K.Chu
Department of Physics and Materials Science, City University of HongKong, Kowloon, Hongkong

I. INTRODUCTION

Electron cyclotron resonance (ECR) plasma, with high density and rich activation radicals, has been extensively used in the surface treatment processing of materials [1-4]. Additionally, ECR plasma has been widely applied in ion sources and semiconductor processes as a result of its relatively high degree of ionization in the low-pressure range in comparison with other conventional discharges [5-8]. ECR plasma is also as a powerful plasma source for plasma immersion ion implantation (PIII) because of its relatively high plasma density and less contamination in the plasma [9-11].

Plasma immersion ion implantation has traditionally been conducted as ion implantation in materials processing, but the modified layer is very thin due to the ion implantation energy limitation. Moreover, the high voltage pulse modulator is expensive and the pulse duty cycle is low, thereby making PIII not suitable for the majority of industrial applications. Hence recently, medium temperature (or medium-frequency) PIII has been developed to form a thicker modified near-surface layer by combining thermal diffusion with ion implantation. The results of this process with regard to nitriding of aluminum and austenitic stainless steel are quite promising [12-14].

In this paper, an ECR PIII device developed for the hydrogen ion implantation of silicon excluding the high voltage pulse power supply will be described. The plasma density is measured with a Langmuir probe. The medium-frequency pulse power supply specially developed for medium-temperature PIII is also presented. The medium-frequency ECR PIII process enhances diffusion and our experimental results to form a gradient transit-layer between the DLC coatings and Ti-6Al-4V biomaterials are reported here.

II. ECR PIII DEVICE

The schematic diagram of the ECR plasma immersion ion implantation (PIII) device is shown in Figure 1. There are six major parts of this device: (1) microwave generator and transmitted system, (2) permanent magnets and auxiliary magnetic coils, (3) vacuum chamber (including resonance cavity and sample chamber) and pumping system, (4) target temperature measuring system, (5) target support, (6) medium-frequency pulse power supply.

The power of the microwave generator with frequency 2.45GHz is adjustable from 100 to 5000 W. The microwave produced by the generator is transmitted into the wave-guide. There is a coupling tuner on the wave-guide to monitor the incoming and reflecting microwave power and the coupling is adjusted by the stubs. The microwave mode is transformed from TE_{10} to TM_{01} and then effectively coupled into a resonant cavity through the quartz window. The resonant zone has a complex shape due to the multi-cusp magnetic configuration formed with the permanent magnets and electromagnetic field produced by the external coil current. Furthermore, the resonant location and zone can be changed relatively by varying the current in the auxiliary magnetic coils on the bottom of the vacuum chamber to control the plasma in the resonant cavity.

The plasma generated in the resonant cavity diffuses into the sample chamber guided by the magnetic field produced by the auxiliary magnetic coils. The other purpose of the guided magnetic field is to control the plasma divergence in order to change the plasma density and uniformity near the target. The target temperature is monitored in-situ with an electrically-floating thermocouple connected directly to the target.

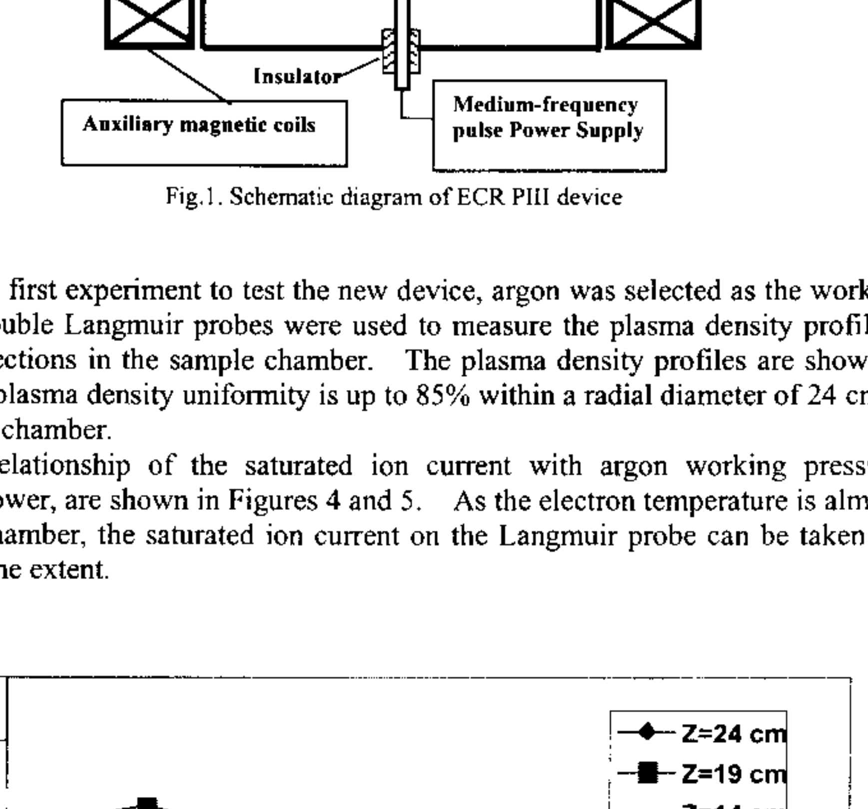

Fig.1. Schematic diagram of ECR PIII device

In our first experiment to test the new device, argon was selected as the working gas. The single and double Langmuir probes were used to measure the plasma density profile in the radial and axial directions in the sample chamber. The plasma density profiles are shown in Figures 2 and 3. The plasma density uniformity is up to 85% within a radial diameter of 24 cm at Z = 24 cm in the sample chamber.

The relationship of the saturated ion current with argon working pressure and input microwave power, are shown in Figures 4 and 5. As the electron temperature is almost constant in the sample chamber, the saturated ion current on the Langmuir probe can be taken as the plasma density to some extent.

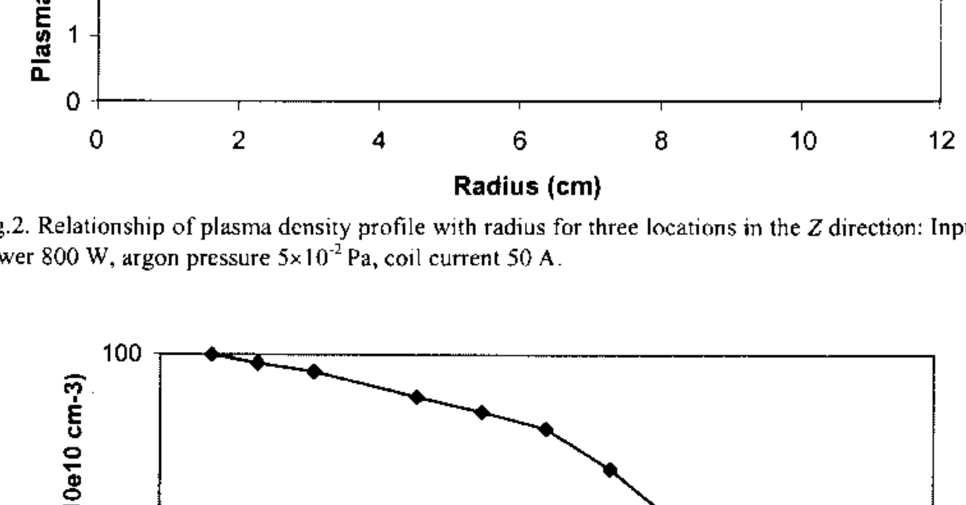

Fig.2. Relationship of plasma density profile with radius for three locations in the Z direction: Input microwave power 800 W, argon pressure 5×10^{-2} Pa, coil current 50 A.

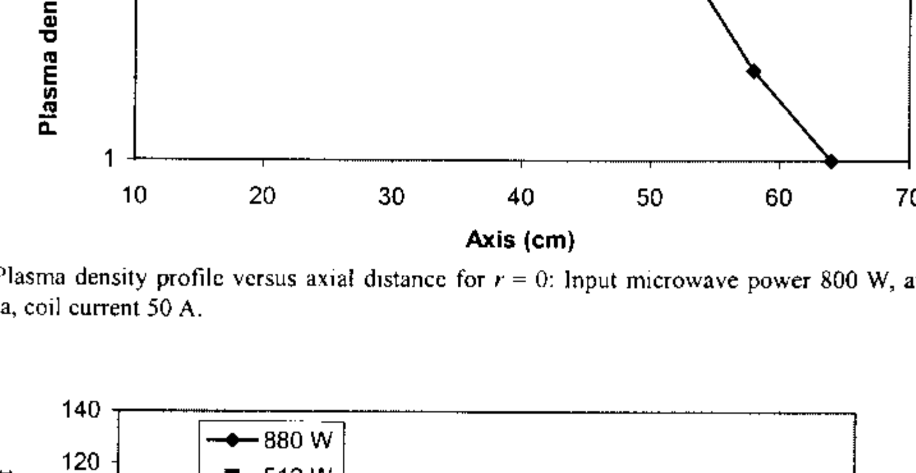

Fig. 3. Plasma density profile versus axial distance for r = 0: Input microwave power 800 W, argon pressure 5×10^{-2} Pa, coil current 50 A.

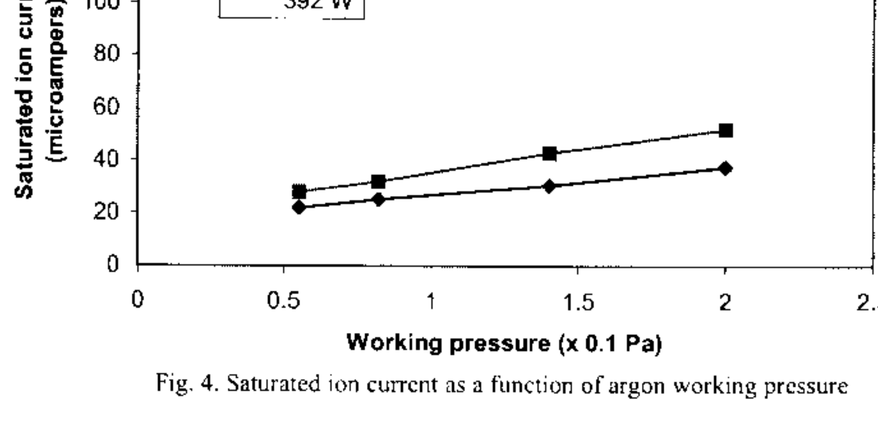

Fig. 4. Saturated ion current as a function of argon working pressure

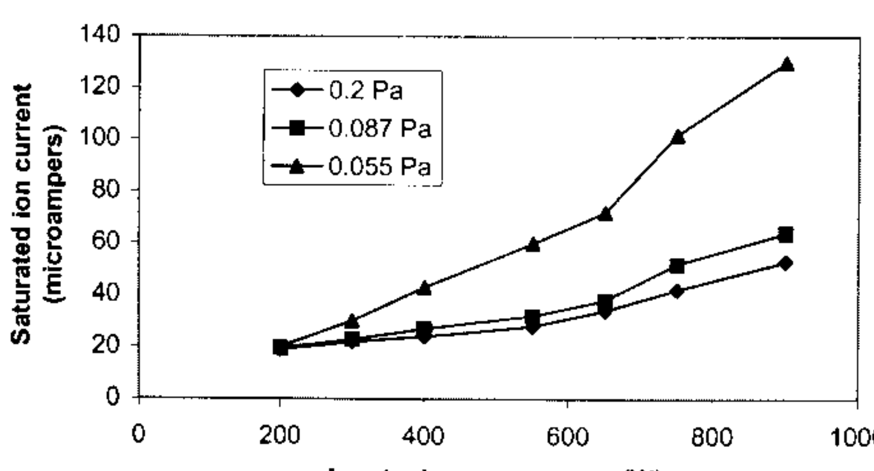

Fig. 5. Saturated ion current as a function of input microwave power

III. MEDIUM-FREQUENCY PULSE POWER SUPPLY

A new medium-frequency square pulse power supply has been developed specifically for this device. The circuitry of the pulse power supply is shown in Figure 6. It essentially consists of high voltage transformer, IGBT, signal control, and protection circuit. The pulse duration and repetition frequency are easily adjustable using the control circuit. The main specifications of the power supply are:
maximum voltage 1.5 kV, repetition frequency 20-40 kHz, pulse width 15-30 μs. The ideal voltage waveform is shown in Figure 7.

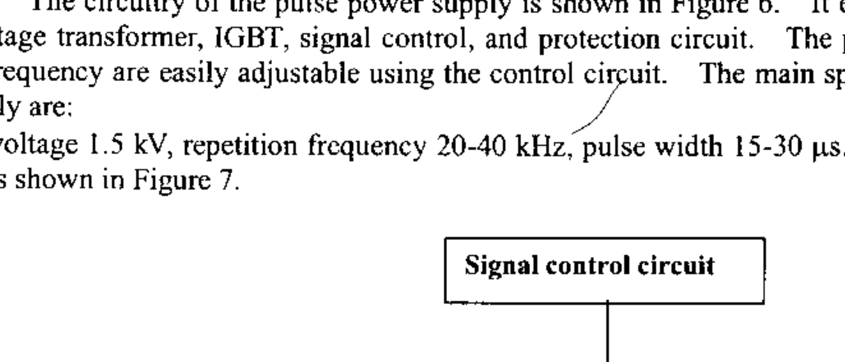

Fig. 6. Circuit schematic of medium-frequency pulse power supply

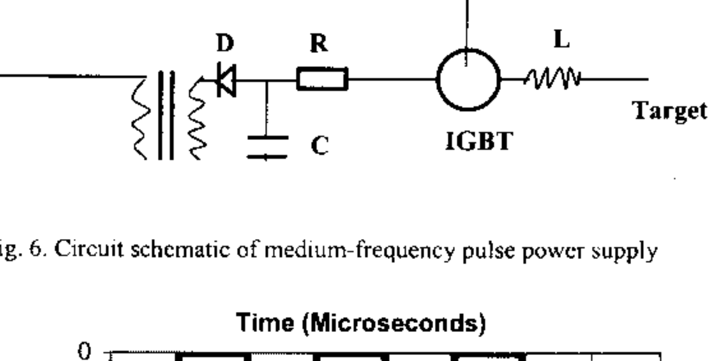

Fig. 7. Typical voltage waveform of pulse power supply

IV. EXPERIMENTAL

Annealed Ti-6Al-4V alloy 5 mm in thickness was machined into disks 25 mm in diameter. The samples were polished to a mirror finish using 0.03-μm alumina paste and ultrasonically cleaned in acetone followed by alcohol for 10 minutes.

Medium-frequency ECR PIII was carried out in the device described above. Firstly, the samples were heated by the electrical heater installed in the target support to about 250°C before pre-cleaning using argon plasma. The heater was then turned off, and the argon plasma was generated in the resonant cavity and the 25 KHz pulse power supply with a maximum voltage of 1.2 kV was applied to the samples. This step was for pre-cleaning and also raised the sample temperature to about 300°C. This step made the starting temperature the same as the that in the rest of the process. Finally, the methane plasma was produced and a negative square pulse bias was applied to the sample. In order to keep the temperature relatively constant in the process, the plasma density was adjusted by changing the coupling microwave power.

The treatment parameters were: base pressure 4×10^{-4} Pa, methane working pressure 6×10^{-2} Pa, methane plasma density near the samples (1~4) $\times10^{10}$ cm^{-3}, sample temperature 300±20°C, maximum voltage -1.2 kV, repetition frequency 25 kHz, pulse width 20 μs, duty cycle 50%, treatment time 90 minutes.

V. RESULTS AND DISCUSSION

The carbon concentration profile and chemical composition versus depth in the near surface were characterized by x-ray photoelectron spectroscopy (XPS). The carbon depth profile is shown in Figure 8.

Two regions can be observed, a decrease in the carbon concentration from 16% in the near surface region and a local maximum with a carbon concentration of about 14% at 20 nm. The buried carbon profile is believed to be due to ion implantation whereas the surface feature is a result of plasma enhanced surface diffusion. It should be noted that it is more difficult to achieve deep carbon diffusion compared to plasma nitriding.

XPS analyses of Ti 2p and C 1s binding energies were performed at two depths, 7.5 nm and 20 nm, and the spectra are displayed in Figures 9 and 10, respectively. It can be observed that the TiC phase exists at both depths, but there is more titanium oxidation in the diffusion zone.

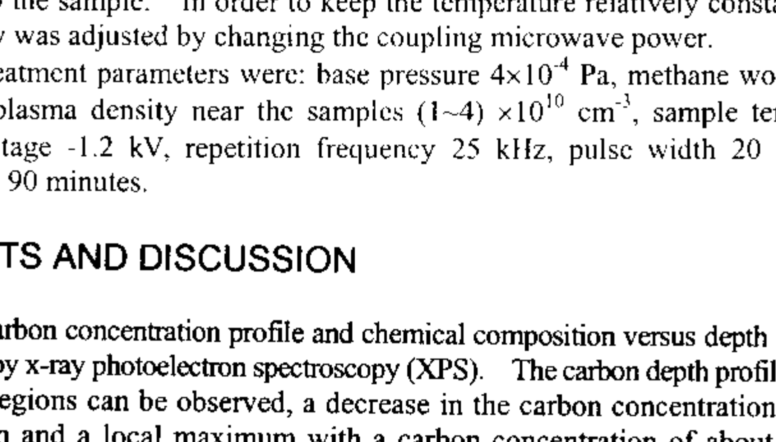

Fig. 8. Carbon concentration profile with depth

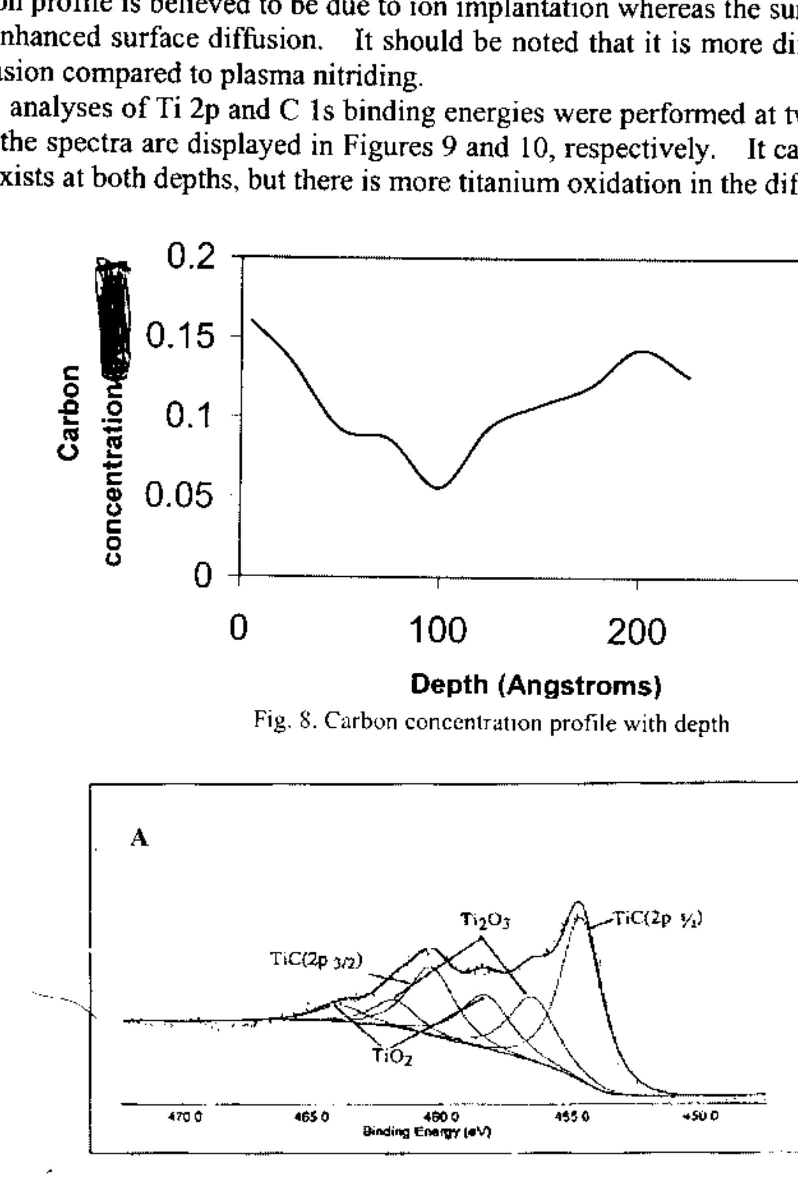

Fig. 9. XPS binding energy spectra in Ti 2p region at the various depth: (A) 7.5 nm; (B) 20 nm.

It is also evident that the relative TiC peak heights are quite different. Coupled with TRIM simulation, the results suggest that only a thermal process occurs in the diffusion zone.

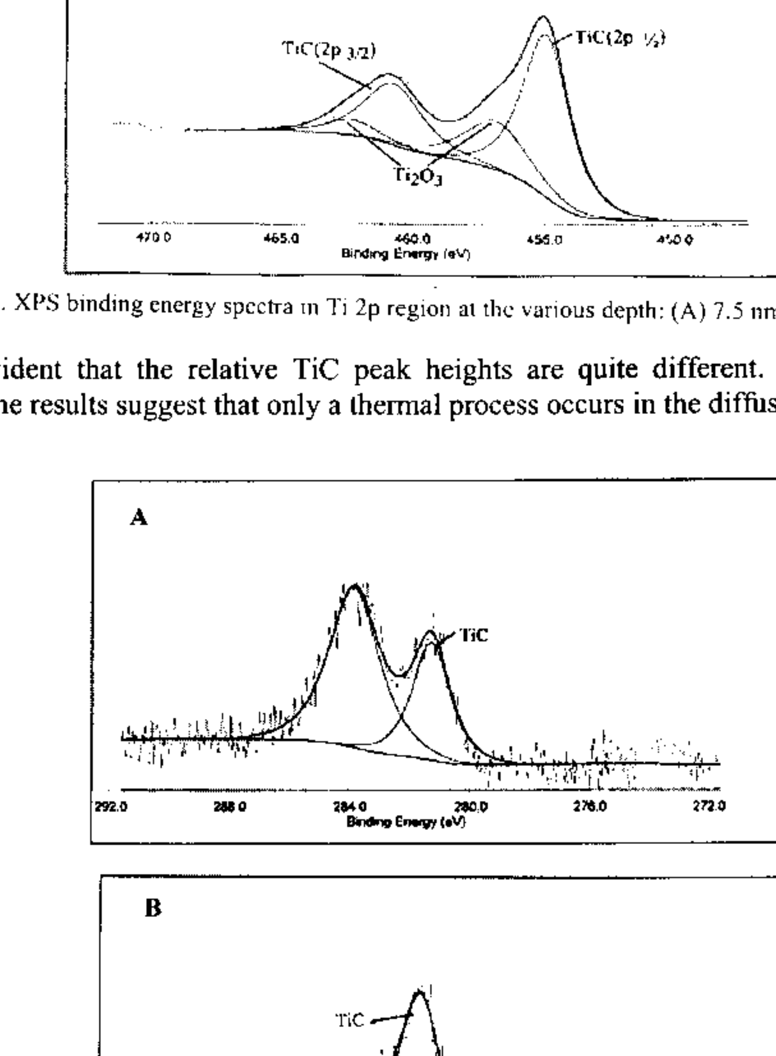

Fig. 10. XPS binding energy spectrum in C 1s region at various depths: (A) 7.5 nm; (B) 20 nm.

VI. CONCLUSION

A novel ECR PIII device and medium-frequency pulse power supply have been successfully developed and the main plasma parameters in the sample chamber have been measured. Our results indicate that this device can produce denser plasma in comparison with other means and it is easier to achieve plasma uniformity over a large area. Our preliminary results of the medium-frequency microwave PIII shows that if the treatment time is longer or the target temperature is higher, it is possible to make the gradient transit-layer for DLC coatings on Ti-6Al-4V biomaterials. It is thus a cost-effective method having a high industrial potential.

ACKNOWLEDGMENTS

The authors wish to acknowledge the contributions of Zeng Xuchu and Mu Lilan. This work was jointly supported by National Nature Foundation of China, grant number 19975014, Hong Kong RGC CERG 9040498 or CityU 1032/00E, Hong Kong RGC – Germany Joint Scheme # 9050150, and City University of Hong Kong SRG 7001177.

[1] Camps Enrique, Becerril, Fernando, Muhl, Stephen, Alvarez-Fregoso O., Villagran M., Thin Solid Films, 373(2000) 293.
[2] Asmussen. Jes Jr., Grotjohn, timothy A., Mak. PengUn, Perrin. Mark A., IEEE Transactions on Plasma Science, 25(1997) 1196.
[3] Sun Jian, Wu Jiada, Zhong Xiaoxia, Lai Bing, Ding Xunmin, Li Fuming, Chinese Journal of Semiconductor, 21(2000) 1019.
[4] Jeon Bup-ju, Jung Il-Hyun, Oh In-Hwan, Lim Tae-Hoon, Kang Moon-sang, Proceedings of the 1996 Conference on Optoelectronic & Microelectronic Materials and Devices, Dec8-11, 1996,Canberra, Aust.
[5] Dalal Vikram L., Maxson Tim, Han Kay, Haroon Sohail, Journal of Non-Crystalline Solids, 227(1998) 1257.
[6] Takada Toshiaki, Sasaki Kimihiro, Electronics and Communications in Japan, Part II: Electronics, 83(2000) 52.
[7] Yoon S.F., Tan K. H., Rusli, Ahn J., Huang Q.F., Diamond and Related Materials, 9(2000) 2024.
[8] Zhang Jinsong, Ren Zhaoxing, Liang Rongqing, Sui Yifeng, Liu Wei, Vacuum Science and Technology, 20(2000) 166.
[9] Rusli, Yoon S.F., Yang H., Ahn J., Surface and Coatings Technology, 123(2000) 134.
[10] Rinner M., Volz K., Ensinger W., Assmann W., Rauschenbach B., Surface and Coatings Technology, 100(1998) 366.
[11] Ikegami T., Grotjohn T., Reinhard D., Asussen J., Proceedings of the 1997 IEEE International Conference on Plasma Science, May 19-22, 1997, San diego, CA, USA.
[12] Liu J., Iyer S.S.K., Min J., Chu P., Gronsky R., Hu Ch., Cheung N.w., Proceedings of the1995 MRS Sprting meeting, Apr 17-20, 1995, San Francisco, CA, USA.
[13] 12. N. Duez, B. Mutel, O. Dessaux, P. Goudmand, J. Grimblot, Surface and Coatings Technology, 125(2000) 79.
[14] X.B. Tian, Z.M. Zeng, T. Zhang, B.Y. Tang, P.K. Chu, Thin Solid Films, 366(2000) 150.